

Article

Not peer-reviewed version

Integrating Synthetic Aperture Radar (SAR) Sentinel 1A and CROPGRO Peanut Simulation Model for Spatial Yield Gap Analysis

[Thirumeninathan Subramanian](#)^{*}, [Pazhanivelan Sellaperumal](#)^{*}, [Sudarmanian N.S.](#), [Ragunath K.P.](#),
Kumaraperumal Ramalingam, [Srinivasan G.](#), Mohan R

Posted Date: 23 January 2023

doi: 10.20944/preprints202301.0401.v1

Keywords: SAR; Sentinel-1A; DSSAT CROPGRO; Peanut; Yield gap



Preprints.org is a free multidiscipline platform providing preprint service that is dedicated to making early versions of research outputs permanently available and citable. Preprints posted at Preprints.org appear in Web of Science, Crossref, Google Scholar, Scilit, Europe PMC.

Copyright: This is an open access article distributed under the Creative Commons Attribution License which permits unrestricted use, distribution, and reproduction in any medium, provided the original work is properly cited.

Article

Integrating Synthetic Aperture Radar (SAR) Sentinel 1A and CROPGRO Peanut Simulation Model for Spatial Yield Gap Analysis

Subramanian Thirumeninathan ^{1,*}, Sellaperumal Pazhanivelan ^{2,*}, N. S. Sudarmanian ³, Kaliaperumal Ragunath ², Ramalingam Kumaraperumal ⁴, Govindasamy Srinivasaan ⁴ and Mohan Ramalingam ¹

¹ Department of Agronomy, Pandit Jawaharlal Nehru College of Agriculture and Research Institute, Pondicherry University, Karaikal - 609 607, Pondicherry (U.T), India; mohankkl@gmail.com

² Water Technology Center, Tamil Nadu Agriculture University, Coimbatore - 638 401, Tamil Nadu, India; ragunathkp@tnau.ac.in

³ ICAR – Krishi Vigyan Kendra, Tamil Nadu Agriculture University, Aruppukottai - 626 101, Tamil Nadu, India; sudarnsagri@gmail.com

⁴ Department of Remote Sensing and GIS, Tamil Nadu Agriculture University, Coimbatore - 638 401, Tamil Nadu, India; kumaraperumal.r@gmail.com (R.K.); srinivasan993.sv@gmail.com (G.S.)

* Correspondence: pazhanivelans@gmail.com (S.P.); thirumeni95@gmail.com (S.T.)

Abstract: Crop yield data is critical for managing agriculture sustainably and assessing national food security. Current study aims to increasing current level of Peanut productivity by analyzing the yield gap of production potential between theoretical yield and actual farmers' yields. The spatial yield gap of Peanut for Thiruvannamalai district of Tamil Nadu is examined in this paper by integrating the products of microwave remote sensing (SAR Sentinel-1A) with DSSAT CROPGRO peanut simulation model. CROPGRO Peanut model was calibrated and validated by conducting field experiment at Oilseeds Research Station, Tindivanam during *Rabi* 2019 for predominant cultivars viz. TMV 7, TMV 13, VRI 2 and G 7. Actual attainable yield was recorded by organizing CCE with help of Department of Agriculture Economics and Statistics in the respective monitoring Villages. Regression analysis between maximum recorded DSSAT Leaf Area Index (LAI) at peak flowering stage of peanut and yield recorded by Crop Cutting Experiment (CCE) for spatial yield estimation of Peanut in Thiruvannamalai district of Tamil Nadu during *Rabi* 2021 was carried out using ArcGIS 10.6 software. The DSSAT CROPGRO simulated potential yield ranged from 3194 to 4843 kg/ha, whereas actual yield ranged from 1228 to 3106 kg/ha, with a considerable disparity between the actual and potential yield levels (1217 to 2346 kg/ha) of the monitored locations. The minimum, maximum and average yield gaps in Peanut for Thiruvannamalai district was assessed as 1890, 2324 and 2134 kg/ha, respectively. To minimize the production difference (Yield gap) of Peanut cultivation, farmers should focus more on management issues such as time of sowing, irrigation or water management, quantity and sources of nutrients, cultivar selection and availability of quality seeds tailored to each region.

Keywords: SAR; Sentinel-1A; DSSAT CROPGRO; peanut; yield gap

1. Introduction

To bridging the yield gap, especially in developing nations, is a strategic step for alleviating the problem of food security. The difference between the actual yield that farmers are currently producing and the potential yield that could be obtained by utilizing the best agronomic methods is known as the yield gap. This can aid in predicting future crop results for specific places and in identifying the contributing elements to the disparity.

In order to discover production barriers, examine measures to enhance agricultural productivity, and identify intervention regions, it is vital to quantify crop yield gaps and assessing food security of nation [1–3]. Furthermore, accurately assessing productivity, land use pattern and food security requires a thorough investigation of existing yield gaps as well as production limits [4,5].

Production capacity changes of farmland, changes in crop productivity, and current yield differences must all to be analysed holistically to potentially offer for farmers policy decision makers so that they optimize their farm land management systems and boost production of food by limiting additional area expansion [6–8].

Mostly agricultural yield disparities are on two purposes [5], first is to determine the level of yield gap, which is defined as the difference between potential yield (Y_p) and average attainable yields, to be able to determine how much average yields may be raised by management adjustments. The second is to figure out the fundamental factors that lead to yield variations so that policy, research, and extension endeavors can prioritise strengthening land and labour productivity.

Measuring potential yield (Y_p) from the highest farmer yield, field trials, and crop simulation models are the three most prominent approaches for assessing potential yield of crops whilst using yield gap (Y_g) analysis [9,10].

A comprehension of farming practices at various scales and the assessment of production gaps can both be greatly improved by remote sensing approaches. Technological breakthroughs in remote sensing technologies, like multispectral and hyperspectral sensors on drones and geosynchronous orbits (Synthetic Aperture Radar), have expanded the possibility to perceive small and marginal landholding systems at greater spatiotemporal resolutions, allowing a more accurate assessment of crop yields while integrating with simulation models in those areas. Crop simulation modelling and satellite image-based earth observation technologies have advanced to quickly allow for better regional crop yield monitoring and forecasting. Remote sensing has been an effective method for coping with heterogeneity during the past two decades, and it can be used in conjunction with more conventional strategies like field tests and simulation models. In fact, remote sensing using sensors mounted on aircraft or satellites has the capacity to offer observations for a single field throughout each growing season. In order to investigate yield gap variability, remote sensing might augment surveys or field experiments by overcoming geospatial data limitations.

Through the use of data with high spatial and temporal resolutions, the most recently launched sophisticated remote sensing satellites aids us in making precise estimates of crop area and yield. Additionally, enhanced spatial, spectral, and temporal resolution make it easier for us to distinguish between crops [11]. Due to the availability of these high-resolution satellite sensors, software with automated processing chains, and advanced agricultural yield models, reliable information on crop acreage, crop conditions, and yields have now been provided. The accuracy of crop classification is improved by time series satellite data's repeated covering of the cultivated area. [12]. SAR sensors have an especially impressive capability to detect structural changes in crop canopies. Additionally, they can accurately identify the crop type due to their sensitivity to a variety of crop biophysical variables, such as LAI, yield, and canopy height [13].

Crop simulation models are used to simulate potential crop yields which are then compared to actual yields in many yield gap analysis [5]. When potential yield (Y_p) is taken from maximal farmer yield and field studies then there shall be many constraints [14]. In order to figure out Y_p from field experiments, it is quite challenging to establish ideal growth circumstances across the crop growth period for a number of seasons to account for climate change. Corresponding to this, the maximum farmers' yield is determined by individual farmers' estimates, which may incorporate flawed information. On the other hand, crop simulation models are very important because they allow for interconnections between crops, soil, weather, water regimes, and management to generate a more precise estimate of Y_p [5]. Models also account for the unpredictability of weather conditions across many years. Thus, notwithstanding difficulties relating to

parameter estimates or structure functioning, crop simulation models provide the most accurate Y_p for a certain area [4,15,16].

In order to address a wide range of complex agronomic problems at both the local and provincial scale, two distinct advancements remote sensing and crop growth simulation models have been created [17,18]. Despite the fact that these two technologies have frequently been explored independently, there is rising interest in using data from remote sensing to update or enhance agricultural ecosystem model simulations. This is because these two technologies are inherently complementary [19–21].

Understanding the causes of yield gap variability can help to improve site specific land management and yields [22]. However, on a micro level, there is a lack of understanding of reasons for yield gap. This is mainly due to understanding factors limiting agricultural production at a local level have used approaches like, surveys and field experiments [23]. These techniques have spatial data limitations since they use a limited number of randomly selected units and fall short of giving a thorough knowledge of yield gaps at the micro level when considering the variety that can be found even within individual fields and plots [14]. The purpose of this research paper is to work for the potential value of satellite-based microwave remote sensing and crop simulation model to measure and explain crop yield gaps.

2. Material and Methods

2.1. Study area

Thiruvannamalai district comes under Northeastern agro climatic zones of Tamil Nadu with the spread over of 6191 square kilometers and lies between $11^{\circ} 55'$ to $13^{\circ} 15'$ North latitude and $78^{\circ} 20'$ to $79^{\circ} 50'$ East longitude. This district has eighteen blocks consisting of 1067 revenue villages and study area map is presented as Figure 1. The prevailed climate is hot sub humid to semi-arid. The mean annual maximum and minimum temperature are 32.6°C and 22.2°C , respectively. The annual rainfall of the Northeastern zone excluding hills varied from 800-1400 mm and more rainfall was received during Rabi 2020-21. Predominant soil type were red sandy loam and clay loam soil which encourages cultivation of Peanut, rice, blackgram and sesame.

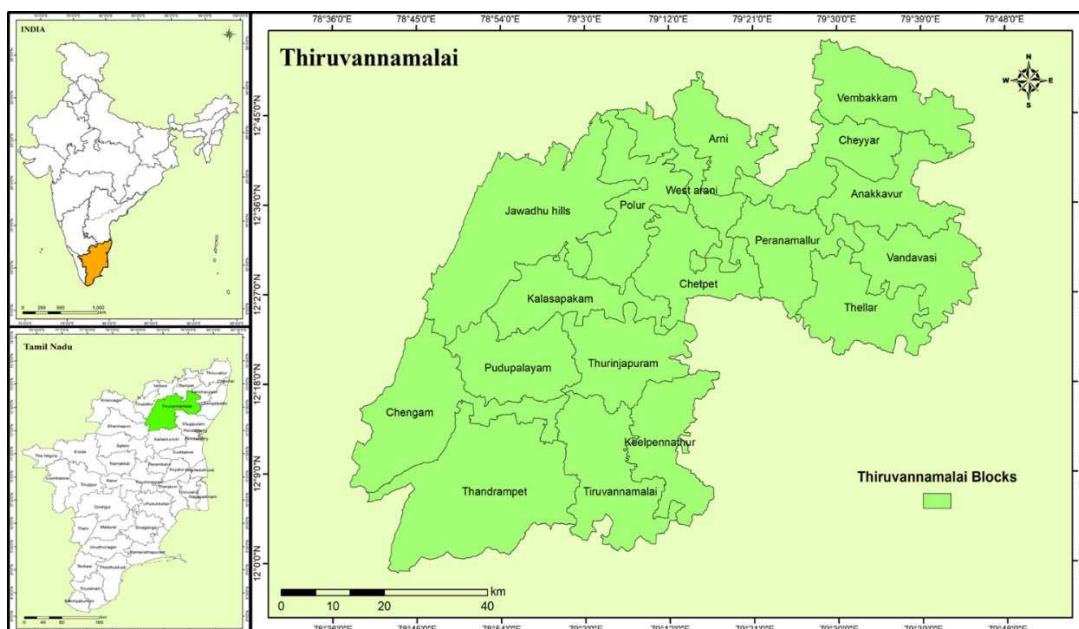


Figure 1. Study area map for Thiruvannamalai district.

2.2. Data used

The benefit of Synthetic Aperture Radar (SAR) is that it can collect data day or night and operates at wavelengths that are not hindered by clouds or poor lighting. With its C-SAR equipment, Sentinel 1A can provide dependable, ongoing wide-area monitoring. Sentinel 1's C-band imaging system features four imaging modes with various resolutions and coverage areas. It is capable of dual polarisation, has a brief revisit time, and delivers products quickly. For crop identification and mapping in the study area during Rabi 2020–21, Ground Range Detected (GRD) information from Sentinel-1A Synthetic Aperture Radar image acquisition with VH polarization in Interferometric Wide (IW) swath mode are gathered at 12-day intervals. The data were downloaded from <https://scihub.copernicus.eu/dhus/> based on the usual Peanut growing season in the research location to have complete coverage during the crop growing season, beginning October 4, 2020, to January 8, 2021.

2.2.1. SAR data processing

The multi-temporal space-borne Sentinel 1A SAR IW-GRD data were converted into terrain-geocoded σ^0 values using an entirely automated processing pipeline created by [24]. The processing string was a module of the MAPscape-RICE programme, created by the Swiss company sarmap. The SAR time series data performed a number of important processing steps, as indicated below and illustrated in Figure 2. to produce terrain geocoded degree values.

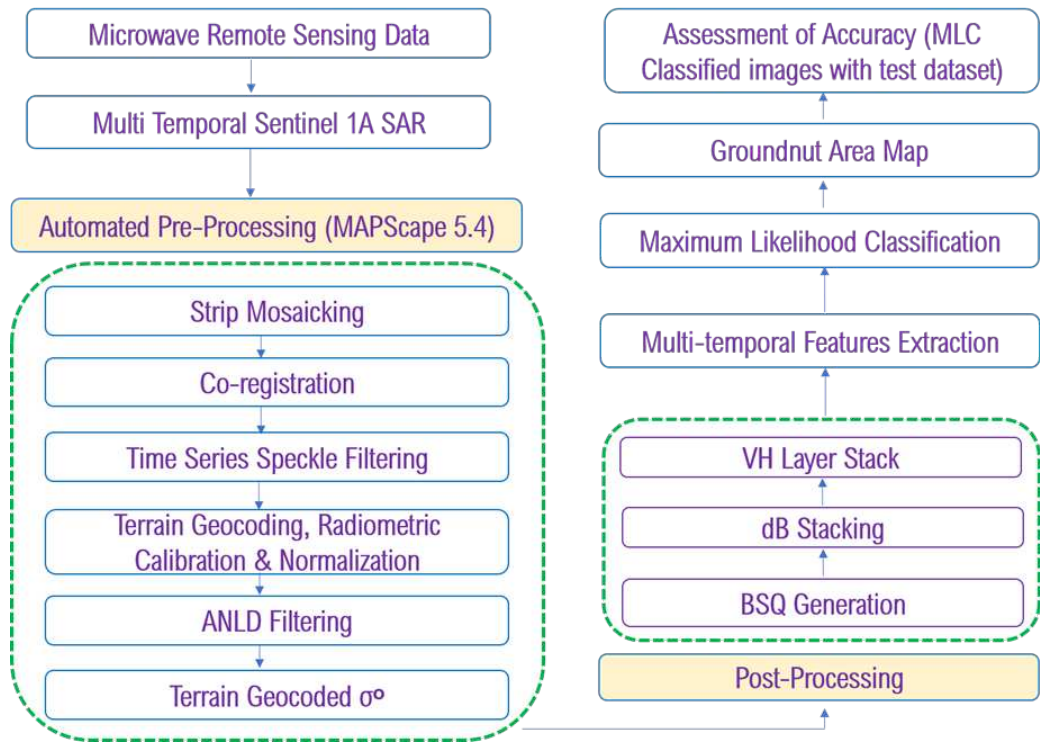


Figure 2. Flow chart for methodology of SAR data processing and Peanut area mapping.

2.3. Crop classification and accuracy assessment

2.3.1. Maximum likelihood classification (MLC)

To classify imaging pixels into a land use / cover category based on pixel value is the purpose of the image classification process. In this work, crop area identification was done using the maximum likelihood

classification (MLC) algorithm. The spectral response pattern is used by the MLC to statistically analyze the individual categories variance and covariance while identifying an unidentified pixel. It is assumed that the training set's distribution is gaussian. According to this premise, the average vector and covariance matrix can completely represent the distribution of a training set for a class. The statistical possibility that a given pixel belongs to a specific class can be calculated assuming these variables.

To determine Peanut, the image was first categorized using MLC with multi-temporal superimposed SAR images. Based on training pixels acquired at various locations, the training spectral signature for Peanut crop was created. The categorization for VH polarization is then completed in order to distinguish the Peanut field from other categories.

2.3.2. Accuracy Assessment

The accuracy of the Peanut area map is validated using the error matrix and kappa statistics. To measure the classification accuracy, each pixel's class assignment in the classified image is contrasted with the matching class assignment on the reference data. An error matrix is created using the agreement and disagreement pixels. The elements of the matrix indicate the number of pixels in the testing dataset, while the columns and rows represent the total number of classes [25]. All of the classified output's classification accuracy was examined.

A farmer survey was used to confirm that the observed post-harvest situation accurately reflected the presence of a Peanut crop during the surveilled season. Generally, the accuracy assessment in fields was performed during the pod filling or maturity phase before harvesting, but in some cases, the field assessment was conducted during post-season and Peanut haulms. The error matrix was used to determine the accuracy metrics, including overall accuracy, producer accuracy, and user accuracy [26]. The proportion of correctly identified cases located along the diagonal, which represent the overall accuracy, were determined as follows:

By dividing the total number of correctly categorized samples by the total number of reference

$$\text{Overall Accuracy} = \frac{\Sigma(\text{Correctly classified classes along diagonal})}{\Sigma(\text{Row Total or Column Total})}$$

samples, the producer's accuracy (errors of omission) for each class was calculated as follows:

$$\text{Producer's Accuracy} = \frac{\text{Number of correctly classified class in a column}}{\text{Total number of items verified in that column}}$$

By dividing the total number of samples in a class that were verified to belong to that class by the number of samples in that class that were correctly classified, the user's accuracy (errors of commission) of each class was calculated as follows:

$$\text{User's Accuracy} = \frac{\text{Number of correctly classified item in a row}}{\text{Total number of items verified in that row}}$$

Kappa Coefficient

The kappa coefficient, which estimates the proportionality (or percentage) increase by the classifier over a simply random assignment to classes, is a different metric for classification accuracy [27]. The formula shown below was used to estimate the kappa coefficient.

$$\hat{K} = \frac{NA - B}{N^2 - B}$$

In the case of a confusion matrix containing r rows and correspondingly r columns, Where,

A = the sum of r diagonal elements, which is the numerator in the computation of overall accuracy

B = sum of the r products (row total x column total)

N = the number of pixels in the error matrix (the sum of all r individual cell values)

2.4. Crop Cutting Experiments (CCEs) for Actual Yield estimation

Actual yield of Peanut or farmers attainable yield during Rabi 2020-21 was estimated with the help of Department of Agriculture Economics and Statistics by organizing CCEs at 31 monitoring sites of Thiruvannamalai district. In each monitoring sites four CCEs were organized at randomly selected area at a size of 5x5 m. The average of Four CCEs from each monitoring site were converted to yield per ha and use it as actual yield for that monitoring site. The estimated yield data used as actual attainable yield for the measure of yield gap.

2.5. Crop simulation using CROPGRO Peanut model for Potential yield estimation

DSSAT is a software package for microcomputers that combines crop, soil, and weather information in common formats for crop modelling and application programme evaluation. The DSSAT was employed in the current analysis because the user may simulate the results of cultivation techniques over a number of years for various crops in any area in the world. The elements of the crop simulation models for DSSAT shown in Figure 3.

In DSSAT version 4.5, the CROPGRO-Peanut model can be utilized to simulate the daily growth and development of the Peanut crop. DSSAT is one-dimensional model that calculates daily variations in soil water content in a single layer through soil evaporation, infiltration, unsaturated flow, irrigation, vertical drainage, root water uptake and plant transpiration. In addition to crop coefficients that were thought to be less variable or even more conservative among crop cultivars, it also required cultivar coefficients (cultivar-specific characteristics) as an input to the model. The model could represent how high temperatures affect peanut development and growth. The maximum potential yield was computed using the input datasets for 31 monitoring locations by DSSAT CROPGRO peanut model. It needed just the mentioned little datasets for its execution.

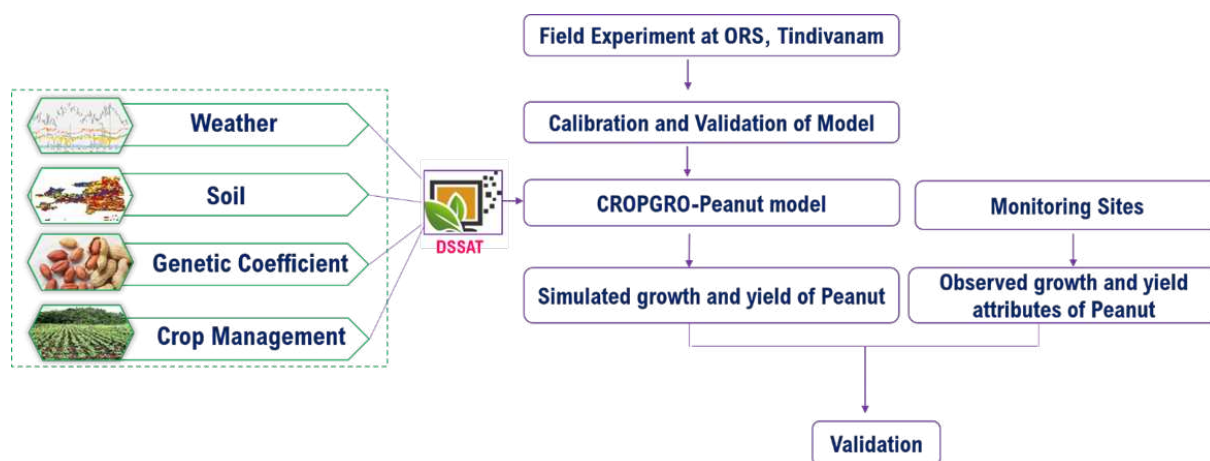


Figure 3. Diagram of database, application and support software components in DSSAT.

2.5.1. Weather file

Automatic Weather Stations (AWS) and regular observatories located at the study districts provided the daily meteorological information on maximum temperature (°C), minimum temperature (°C), solar radiation (MJ m⁻² day⁻¹), and rainfall (mm) for Rabi 2020-21, which were used to create a weather file for

running the CROPGRO-Peanut model. To anticipate the yield, the DSSAT model needed weather information for the whole crop's growing season.

2.5.2. Soil data file

The Department of Remote Sensing and Geographical Information System at the Tamil Nadu Agricultural University in Coimbatore provided the soil data used to create the soil files. This was accomplished by using a digital soil information system that had data on the following soil characteristics (1:50000) viz., depth, texture, pH, EC, BD, drainage, organic carbon, soluble P and K, Ca and Mg, and CEC. The soil profile information's as required in DSSAT were fed into the S-Build tool in DSSAT to create a soil file. The Thiruvannamalai district comprises of 12 soil series viz., Perunthurai, Devikapuram, Pedakallupalli, Meyyur, Vetavalam, Vilukam, Kolathur, Ayyalur, Perumalthangal, Mattathari, Parapperi, Kalugachalapuram and details were used for S build tool presented in Appendix 1.

2.5.3. Crop management file

The inputs to the model for each of the 31 monitoring locations that will be stimulated for Rabi 2020–21 were documented in the crop management (X built) file. The actual figures of the experimental conditions and field characteristics, including the name of the weather station, the soil, the initial soil moisture, the field's description, planting geometries, the conditions of inorganic nitrogen, irrigation and water management, fertilizer management, tillage operations, the application of organic residue and chemicals, environmental modifications, harvest management, simulation control mechanisms (specification of simulation options, such as starting dates, on/off options for water and nitrogen balances, symbiosis) and output options were included in the X built tool as crop management file.

2.5.4. Estimation of genetic co-efficient Peanut

The tweaking of genetic parameters, also known as model calibration or parameterization, ensuring that simulated and observed values are closely comparable. The genetic variables of cultivars were estimated using the data collected from the experiment. In order to achieve the most accurate fit between the observed and simulated number of days to the plant developmental events and grain yield at harvest, the genetic coefficients that affect the occurrence of developmental stages in the CROPGRO-Peanut model entrenched in DSSAT model were derived successively by manipulating the relevant coefficients. For developing varietal genetic coefficient, the field experiment with randomized block design was conducted for popular Peanut varieties at Oilseeds Research Station, Tamil Nadu Agricultural Research Station, Tindivanam during *Rabi* 2019-20 against the ruling varieties viz., TVM 7, TMV 13, VRI 2 and G 7 were used for generating varietal coefficient.

2.6. Yield estimation by integrating Remote Sensing and DSSAT Crop growth model

SAR Sentinel-1A data integrated with DSSAT CROPGRO Peanut for estimating Peanut yield were presented in Figure 4. LAI values retrieved from dB images of the SAR data was used to integrate the DSSAT simulated yield with the remote sensing data. A linear regression equation was generated between DSSAT simulated yield and spatially simulated LAI values for estimating Peanut yield.

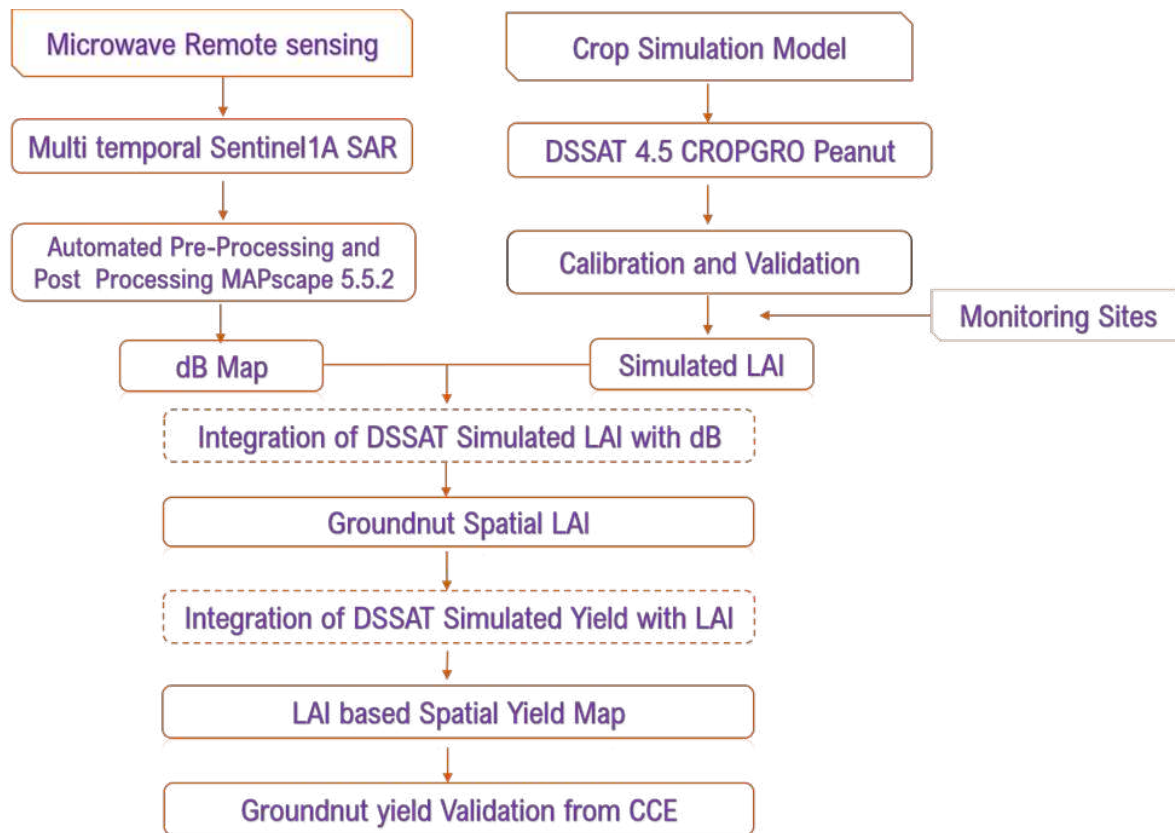


Figure 4. Integration of Remote sensing and DSSAT model for yield estimation.

2.6.1. Generation of LAI for Peanut yield estimation

Five LAI readings were taken from each monitoring field, and the average was calculated. In order to provide information to the CROPGRO-Peanut system for simulation and validation, yield data was collected at the completion of the season from each monitoring field and the entire dataset was finalized over the study area with measurements of Peanut pod yield and LAI. Regression analysis was carried out between the observed and expected yield using the data from the study region pooled into a single dataset.

2.6.2. Retrieving LAI from dB images of SAR data

Using the point sample tool in QGIS 2.18.4, the dB (back scattering) readings of Peanut crops were gathered for monitoring fields. In the monitoring Peanut fields of the study region, the equation for linear regression was created between the dB readings and the simulated LAI values at pod growth stage (Figure 5). The raster calculator tool in ArcMap gives users the option to create selection queries, enter Map Algebra syntax, or do basic arithmetic using operators and functions. Therefore, in this investigation, the dB values of dB pictures from mature stages were substituted for the calculated regression values using the raster calculator in ArcMap. To construct yield maps and statistics spatially, an empirical method was used to extrapolate the field observed and DSSAT calculated LAI values (Figure 6).

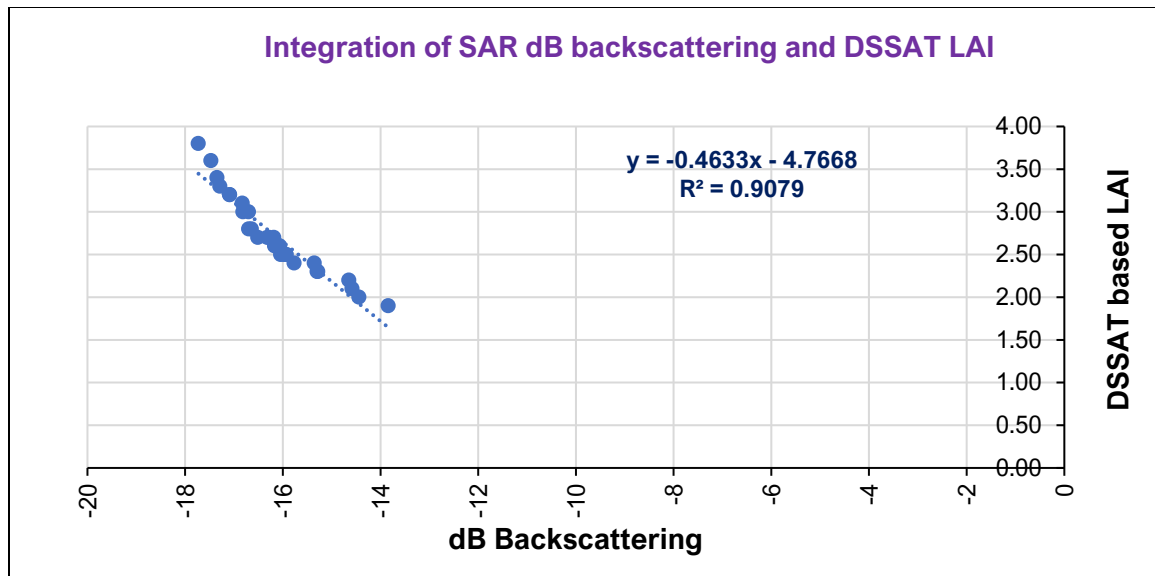


Figure 5. Integration of DSSAT simulated LAI and maximum SAR dB backscattering at pod formation stage.

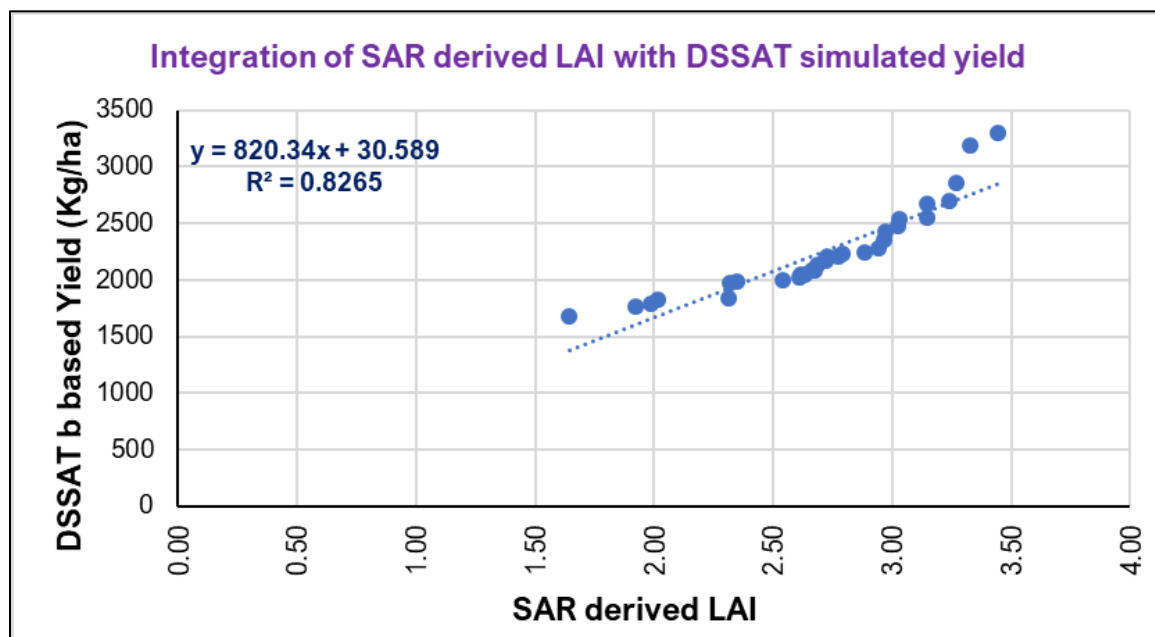


Figure 6. Integration of SAR derived LAI and DSSAT simulated yield for spatial estimation.2.7. Yield Gap estimation.

Yield gap is defined as the difference between potential yield (Y_p) and average yield (Y_a). The potential yield was derived from crop simulation model CROPGRO peanut by a trial conducted at Oilseeds Research Station, Tindivanam. Basic information essential for DSSAT model calibrate and validate were used from this trial and estimated the potential yield of Peanut for the study area. Actual yield data of Peanut were collected by organizing the crop cutting experiments in the study area.

3. Results and Discussion

3.1. Peanut area and accuracy assessment

Peanut area map for the Thiruvannamalai district were derived from multi temporal C-band SAR imagery of Sentinel-1A. Using the shape files of administrative boundaries, district wise and block wise maps and statistics of Peanut area were extracted for 18 blocks of Thiruvannamalai district. The classified Peanut area for each block are displayed in Table 1 and Figure 7 and the total peanut growing area during Rabi 2020-21 was estimated to be 32298 ha. Thandrapet block in Thiruvannamalai district had the maximum area, with 6970 ha followed by Thuringapuram, Thiruvannamalai, Keelpennathur and Chengam blocks, which had 5576, 5197, 4989 and 4111 ha, respectively. The Jawadhu hills block of Thiruvannamalai district recorded a minimum area of 29 ha.

The Peanut area maps were assessed for accuracy on a Peanut or non-Peanut basis, where all other land cover types were grouped into non-Peanut class. In total 103 validation points covering 69 Peanut and 34 non-Peanut points were considered for validation and confusion matrix were presented in Table 2. The overall classification accuracy was 87.4 per cent with a kappa score of 0.75 indicating the accuracy of classification. The Overall accuracy (> 80 per cent) and kappa score (>0.50) indicated that the assessment was of high quality. The results were in accordance with [28–31] has delineated the crop area estimation with high classification accuracy using multi temporal sentinel 1A data had indicated the suitability of remote sensing-based products for crop area estimation and monitoring for policy decisions, including crop insurances.

Table 1. Block-wise Peanut area for Thiruvannamalai district of Tamil Nadu during *Rabi* 2020-21.

S.No.	Block Name	Peanut Area (ha)
1	Anakkayur	57
2	Arani	220
3	Chengam	4111
4	Chetpet	454
5	Cheyyar	171
6	Jawadhu hills	29
7	Kalasapakam	757
8	Keelpennathur	4989
9	Peranamallur	491
10	Polur	216
11	Pudupalayam	2173
12	Thandrapet	6970
13	Thellar	103
14	Thuringapuram	5576
15	Thiruvannamalai	5197
16	Vandavasi	328
17	Vembakkam	36
18	West arani	421
Total		32298

Table 2. Confusion matrix for accuracy assessment for Peanut classification during *Rabi* 2020-21.

	Predicted class from the map		Accuracy (%)
	Peanut	Non-Peanut	
Peanut	59	10	85.5
Non-Peanut	3	31	91.2

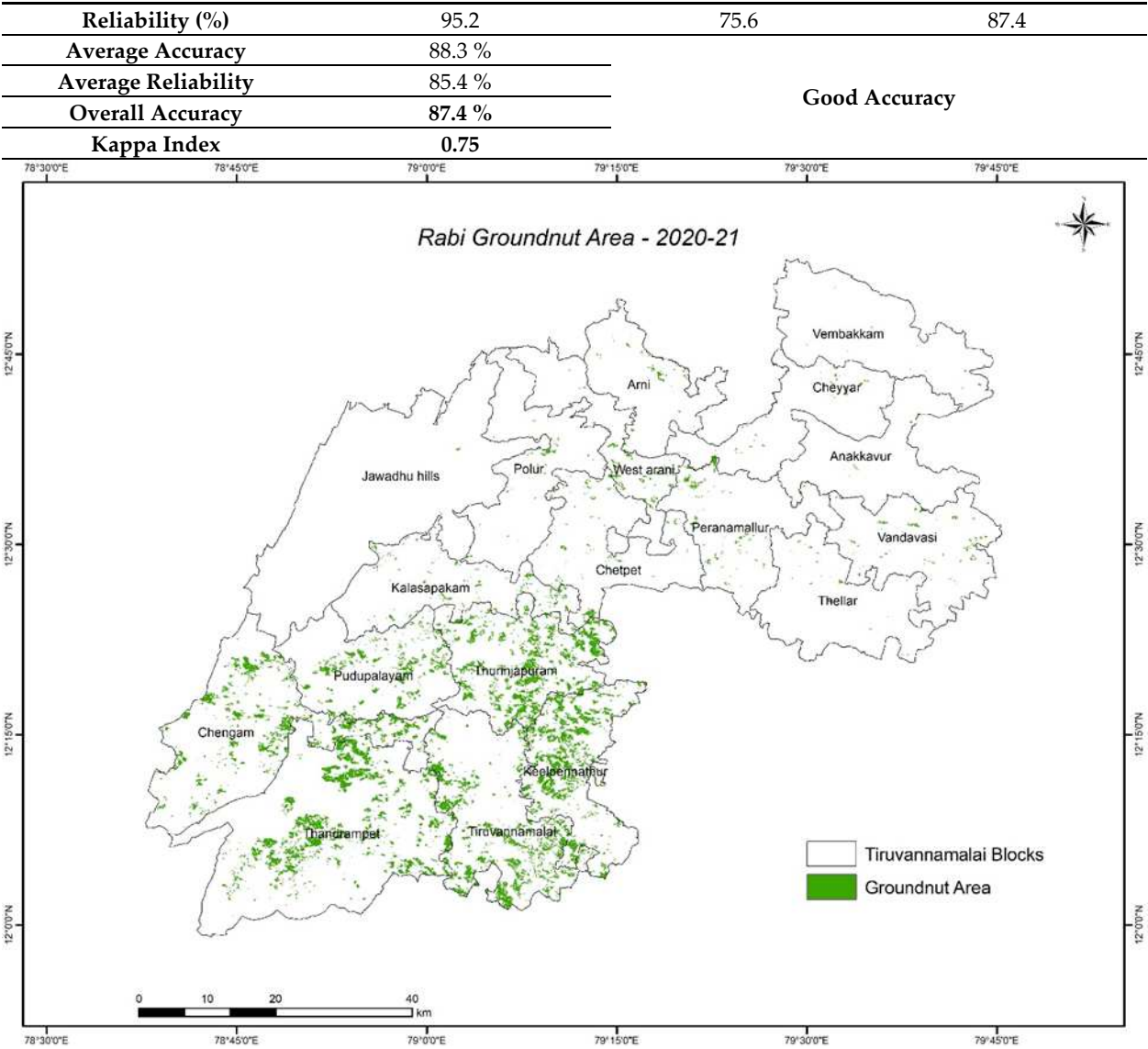


Figure 7. Peanut area of Thiruvannamalai district during Rabi 2020-21.

3.2. Genetic Coefficient development and calibration of DSSAT model

Crop simulation model genetic coefficient development and calibration are vital for establishing their credibility and ability in simulating growth, development, yield attributes and yield of crops [32]. Among the four varietal genetic coefficients (Table 3) generated during the *Rabi* season of 2019-20, the time between emergence to flower appearance (EM-FL) and time between the first flower to first pod (FL-SH) ranged from 17.50 to 19.00 photothermal days and 7.00 to 8.00 photothermal days, respectively. In contrast, the time between the first flower to first seed (FL-SD) and the time between first seed to physiological maturity stage (SD-PM) was found to be a range of 17.30 to 18.50 and 58.00 to 62.00 photothermal days, respectively. The maximum leaf photosynthesis rate ranged from 1.09 to 1.25 mg CO₂ m⁻² s⁻¹. The Seed filling duration (SFDUR) and seeds per pod ranged from 31 to 33 photothermal days and 1.65, respectively, for six varieties. Similarly, [33–36] developed genetic coefficient for groundnut cultivars to various agro climatic zones of India for yield estimation using simulation models.

Table 3. Developed genetic coefficient for ruling varieties of Peanut at Thiruvannamalai district of Tamil Nadu.

Sl. No	Codes	Genetic coefficient	TMV7	TMV13	VRI2	G7
1.	CSDL	Critical short-day length below which reproductive development progresses with no day length effect (for short-day plants) (hour)	11.84	11.84	11.84	11.84
2.	PPSEN	Slope of the relative response of development to photoperiod with time (positive for short day plants) (1/hour)	0.00	0.00	0.00	0.00
3.	EM-FL	Time between plant emergence and flower appearance (R1) (photothermal days).	17.50	18.50	18.30	19.00
4.	FL-SH	Time between first flower and first pod (R3) (photo thermal days)	8.00	7.00	7.50	7.30
5.	FL-SD	Time between first flower and first seed (R5) (photo thermal days)	18.00	17.50	17.30	18.50
6.	SD-PM	Time between first seed (R5) and physiological maturity (R7) stages (photothermal days)	58.00	62.00	59.00	61.30
7.	FL-LF	Time between first flower (R1) and end of leaf expansion (photothermal days)	67.00	70.00	68.00	69.50
8.	LFMAX	Maximum leaf photosynthesis rate at 300 C, 350 vpm CO ₂ , and high light (mgCO ₂ /m ² /s)	1.09	1.11	1.16	1.25
9.	SLAVR	Specific leaf area of cultivar under standard growth conditions (cm ² /g)	245	228	259	263
10.	SIZLF	Maximum size of full leaf (three leaflets) (cm ²)	16.00	16.00	16.00	16.00
11.	XFRT	Maximum fraction of daily growth that is partitioned to seed + shell	0.72	0.75	0.73	0.70
12.	WTPSD	Maximum weight per seed (g)	0.38	0.37	0.39	0.41
13.	SFDUR	Seed filling duration for pod cohort at standard growth conditions (photothermal days)	31.00	33.00	32.50	33.00
14.	SDPDV	Average seed per pod under standard growing conditions (#/pod)	1.65	1.65	1.65	1.65
15.	PODUR	Time required for cultivar to reach final pod load under optimal conditions (photothermal days)	17.30	19.00	18.00	19.20
16.	THRSH	The maximum ratio of (seed/(seed+shell)) at maturity (Threshing percentage)	71.00	74.00	77.00	79.00
17.	SDPRO	Fraction protein (g) per g seed	0.27	0.27	0.27	0.27
18.	SDLIP	Fraction oil (g) per g seed	0.51	0.51	0.49	0.48

The capability of the DSSAT CROPGRO peanut model to predict growth and development of the four predominant Peanut cultivars viz. TMV7, TMV13, VRI 2 and G7 (Table 4) were assessed to predict crop response as influenced by season, weather, management and soil distribution by field experiment conducted at Oilseeds Research Station, Tindivanam.

Table 4. Growth and development variables simulated by DSSAT- CROPGRO Peanut on ruling varieties cultivated in study area.

Sl.No	Variables	TMV7	TMV13	VRI2	G7
1.	Anthesis day (dap)	26	26	26	26
2.	First pod day (dap)	34	36	38	38
3.	First seed day (dap)	44	44	44	45
4.	Physiological maturity day (dap)	103	96	101	101

5.	Yield at harvest maturity (kg [dm]/ha)	2908	2877	3476	3353
6.	Pod/Ear/Panicle weight at maturity (kg [dm]/ha)	4098	3935	4657	4577
7.	Number at maturity (no/m ²)	1274	1053	1159	1047
8.	Unit weight at maturity (g [dm]/unit)	0.23	0.27	0.30	0.32
9.	Number at maturity (no/unit)	1.58	1.6	1.6	1.62
10.	Tops weight at maturity (kg [dm]/ha)	10537	10195	11176	10941
11.	By-product produced (stalk) at maturity (kg[dm]/h)	7630	7320	7700	7590
12.	Leaf area index	4.93	5.37	5.38	5.20
13.	Harvest index at maturity	0.276	0.282	0.311	0.306
14.	Threshing % at maturity	70.95	73.11	74.65	73.27
15.	Grain N at maturity (Kg ha ⁻¹)	143	140	176	168
16.	Tops N at maturity (Kg ha ⁻¹)	277	270	306	297
17.	Stem N at maturity (Kg ha ⁻¹)	52	50	50	48
18.	Grain N at maturity (%)	4.93	4.87	5.06	5
19.	Tops weight at anthesis (kg [dm]/ha)	429	528	372	495
20.	Tops N at anthesis (Kg ha ⁻¹)	14	17	11	15
21.	Leaf number per stem at maturity	24.92	26.19	24.01	24.76
22.	Grain oil at maturity (%)	50.04	50.38	47.86	46.83
23.	Canopy height (m)	0.65	0.69	0.59	0.56
24.	Emergence day (dap)	8	8	8	7

Further, the DSSAT model resulted in a simulated canopy height of 56 to 69 cm, and the maximum LAI for these six varieties ranged from 4.93 to 5.60. These simulation results were in line with the findings of [37], who opined that when independent crop and soil datasets were used to evaluate, the PNUTGRO model was influenced by seasons and location on simulating growth and yield. Apart from that, [38–40] tried to simulate the varietal influence on the growth and physiological process at different regions using DSSAT crop simulation model. The simulated Peanut pod yield of different Peanut varieties ranged from 3935 to 4657 kg ha⁻¹. Accordance with [28], simulated the potential yield of rainfed Peanut across major production zones of Tamil Nadu, which correlated highly with the results obtained in the present study among the varieties. Similar finding on pod yield simulation by DSSAT in a different location was reported by [36,37,41–43] and simulation model overestimated the pod yield then actual attainable yield because simulation of crops has been simulated the yield without limiting factors. The CROPGRO peanut model was used by [34] to simulate the phenological events, yield and yield attributing characters of Peanut cultivars of GG 2 and GG 20 in Gujarat precisely. In the past years, many research efforts were taken to simulate the growth and productivity of Peanut and other crops.

3.3. Spatial estimation of Potential, Actual yield and Yield gap in Peanut

3.3.1. Potential Yield Estimation

DSSAT based potential yield for monitoring sites and block wise spatial Peanut potential yield of Thiruvannamalai district were furnished in Tables 5 and 6. According to [44] regression analysis is a useful method for creating yield prediction models. Among the monitoring sites, the maximum potential production of 4843 kg/ha was simulated using CROPGRO peanut at Mel palur and Kil palur villages, while the least potential yield of 3194 kg/ha was simulated at Tandarai village of Thiruvannamalai district. Similarly, from the block wise spatial potential yield of 18 blocks of Thiruvannamalai district, minimum spatially estimated potential yield varied from 3711 to 3805 kg/ha recorded at Pernamallur and Polur blocks, respectively with mean minimum yield of 3750 kg/ha. The maximum spatially estimated potential yield varied from 3936 to 4306 kg/ha recorded at Thandarampet and Vembakkam blocks, respectively with

mean maximum of 4029 kg/ha. The overall mean spatially estimated potential yield for Thiruvannamalai district was 3874 kg/ha and spatially estimated potential yield map was presented in Figure 8.

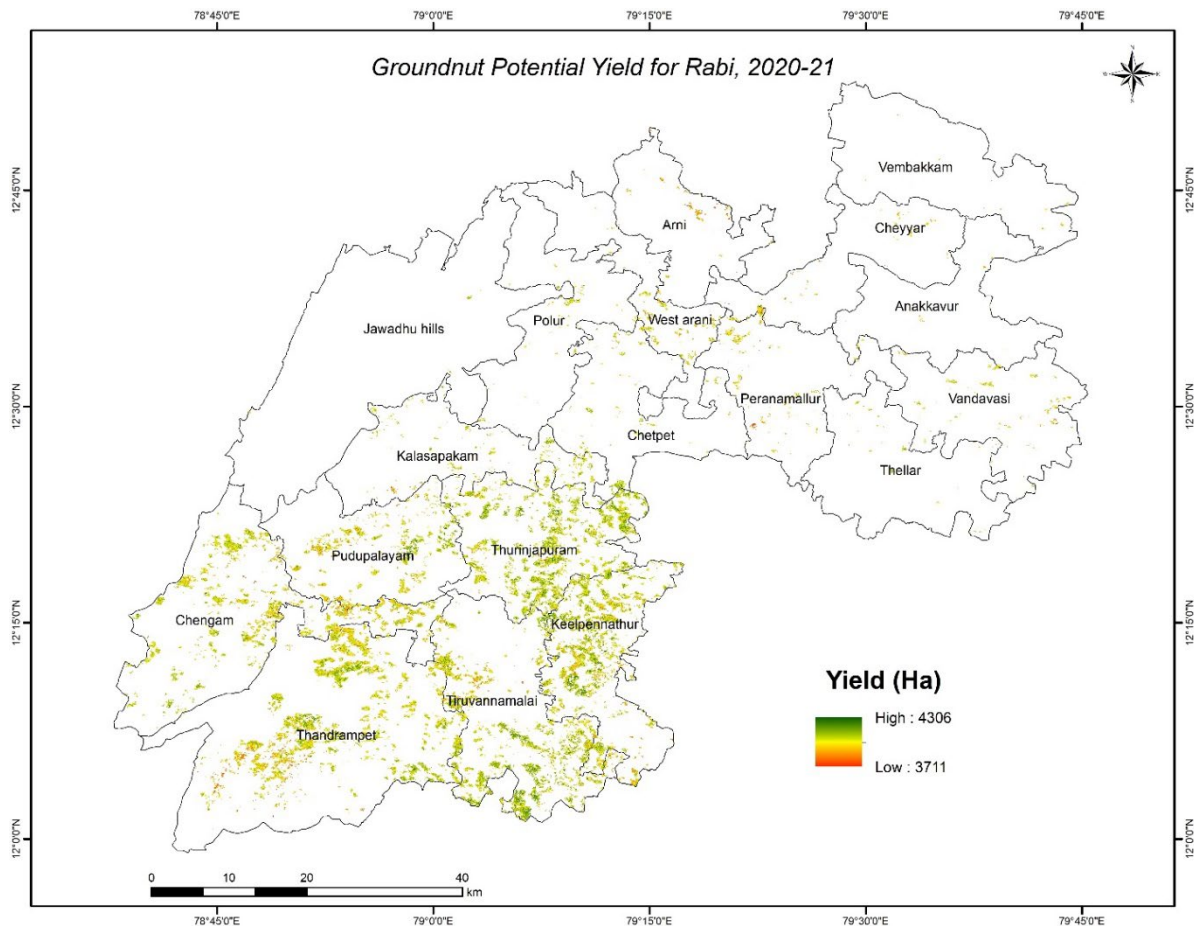


Figure 8. Spatial Peanut potential yield of Thiruvannamalai district during Rabi 2020-21.

As the technique simulates based on given soil, water, climate and management to their full capacity, DSSAT based potential yield estimation always provides higher yield than farmers attainable yield similar to the findings [45]. The DSSAT model simulates daily leaf area index (LAI), vegetation status parameters, biomass production and potential yield using soil, crop management and daily weather data as input. As a result of taking into consideration significant interactions between crops, weather, soil, water regimes, and management, as well as variations in weather across years and areas, simulation models also offer the most precise estimation of potential yield. Within the climatic, soil, and management context of a certain cropping system, they enable assessment of potential or water-limited productivity. Crop models will therefore perform better if provided a technique to incorporate both temporal and spatial variation to the level that data are place specific than any empirical method can do [5].

3.3.2. Actual Yield Estimation

Crop Cutting Experiments (CCE) based actual yield of monitoring sites and block wise spatially estimated actual yields were presented in Tables 5 and 6. Actual Peanut yields recorded at monitoring locations of Thiruvannamalai district during Rabi 2020-21 ranged from 1228 to 3106 kg/ha in Agaram and Mel palur villages, respectively. Among the blocks of Thiruvannamalai district, minimum spatially

estimated actual yields were 1394 to 1644 kg/ha in the Tandarampet and Jawadhu hills blocks, while maximum yields ranged from 1858 to 2526 kg /ha in the Vembakkam and Tandarampet blocks, respectively. The overall mean actual spatial yield was 1740 kg/ha and the actual spatial yield map was presented in Figure 9.

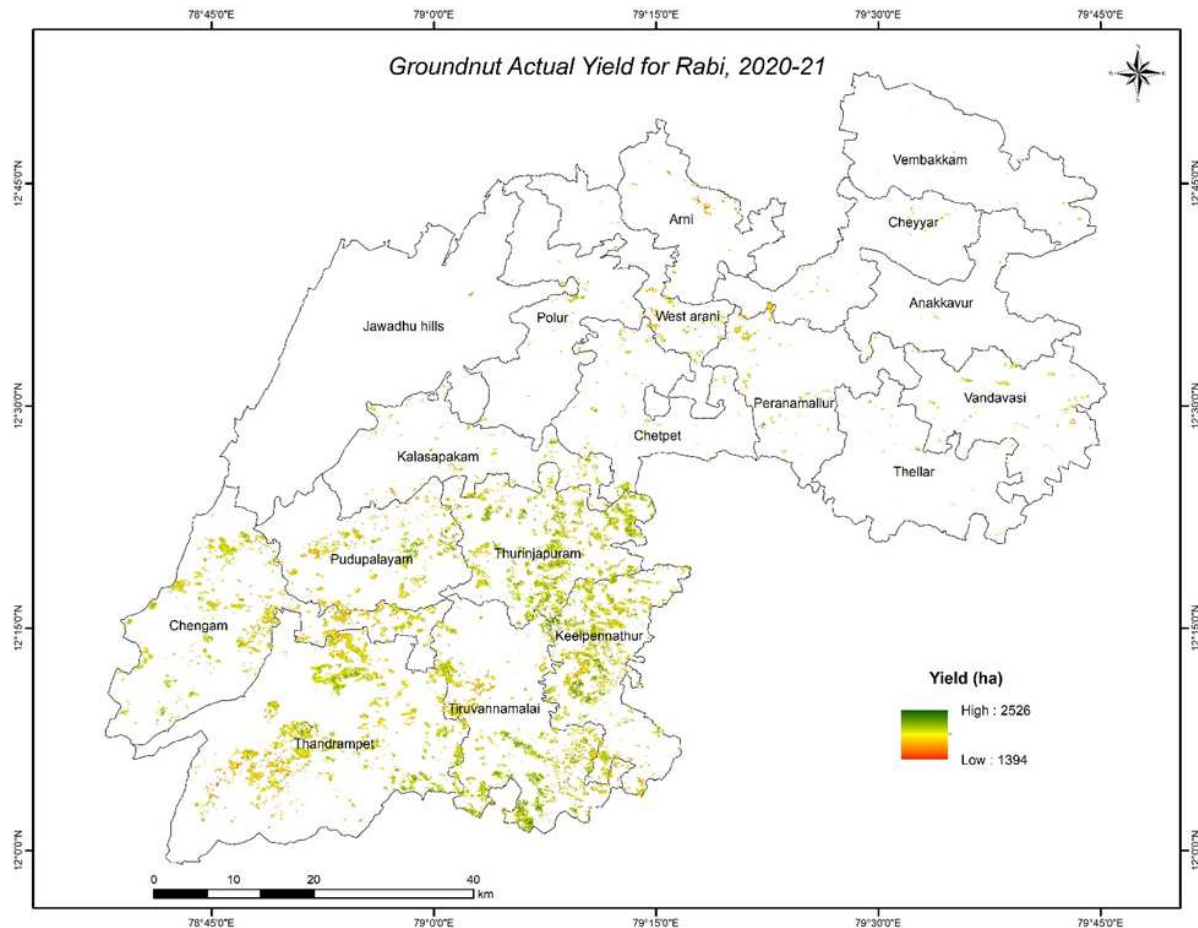


Figure 9. Spatial Peanut actual yield of Thiruvannamalai district during Rabi 2020-21.

During *Rabi* 2020-21, the actual crop actual decreased in comparison to previous years. However, such a decrease on the actual yield was accompanied by a significant year to year fluctuation, which may be attributed to rainfall variability. The existing relationship between crop growth period rainfall and overall actual production is supported by [46]. Although it is still in its early stages, the decline in real yield may be due to a change in the region's adoption of better agronomic measures during the course of the indicated period.

3.3.3. Peanut Yield Gap Estimation

The yield gap of monitoring sites and block wise spatial yield gap are presented in Tables 5 and 6. Among the monitoring sites, Ponnaiyur recorded the more yield gap of 2346 kg/ha whereas Mangalam village recorded the least yield gap of 1217 kg/ha compared to other monitoring sites. For the Thiruvannamalai district, the minimum yield gap ranged from 1456 to 2072 kg/ha at Thiruvannamalai and Vembakkam blocks while the highest yield gap of 2231 to 2508 kg/ha prevailed at Thellar and Thiruvannamalai blocks respectively. The overall mean spatial yield gap of Thiruvannamalai district was

estimated at 2134 kg/ha. By combining remote sensing (SAR Sentinel-1A) data with crop simulation models (DSSAT CROPGRO peanut) the spatial yield gap of Peanut was investigated in this paper for Rabi 2020-21 and yield gap map was presented in Figure 10. The yield gap recorded was 1217 to 2346 kg/ha and the major production constraints of Peanut for yield gap in the district were seasonal rainfall variability, poor soil fertility, lack of improved varieties and inadequate weed managements. The current yield gap could be managed by combining traditional agronomic approaches and latest technologies with involvement of different stakeholders. A substantial amount of work has been devoted to mapping and interpreting yield variations *within* a single field in order to inform precision agriculture applications [4].

Table 5. Peanut Potential, Actual and Yield gap estimation for monitoring sites of Thiruvannamalai district of Tamil Nadu during *Rabi* 2020-21.

Sl. No.	Village Name	Latitude	Longitude	DSSAT based potential Yield	CCE based Actual yield	Yield Gap
1	Agaram	12.60	79.33	3521	1228	2293
2	Ariyalai	12.44	79.16	4607	2829	1778
3	Athurai	12.48	79.25	3521	1408	2113
4	Budhamangalam	12.40	79.22	4607	2718	1889
5	Edakkal	12.08	79.00	4150	2465	1685
6	Isukalikatteri	12.10	79.17	3414	1365	2049
7	Kallanai	12.13	79.18	3414	1496	1918
8	Kambattu	12.12	79.02	4403	2718	1685
9	Karampoondi	12.26	79.18	4607	2985	1622
10	Kil palur	12.42	78.94	4843	2964	1879
11	Konnamadai R.F.	12.09	79.06	4403	2794	1609
12	Kovur	12.40	79.16	3521	1289	2232
13	Malappambadi	12.25	79.13	3521	1428	2093
14	Mallavadi	12.32	79.08	4607	2806	1801
15	Maluvambattu	12.11	79.01	3807	1618	2189
16	Mamandur	12.67	79.33	3521	1456	2065
17	Mangalam	12.34	79.19	3322	2105	1217
18	Mel palur	12.40	78.93	4843	3106	1737
19	Nambedu	12.57	79.47	3521	1369	2152
20	Padiyamputtu	12.39	79.20	4607	2569	2038
21	Ponnaiyur RF	12.19	78.93	3774	1428	2346
22	Puthur	12.77	79.26	3521	1346	2175
23	Radhapuram	12.15	78.96	3774	1659	2115
24	Tandarai	12.12	79.16	3194	1725	1469
25	Thandarampatti	12.15	78.95	3774	1571	2203
26	Tirumalai	12.56	79.20	3521	1342	2179
27	Vallivagai	12.29	79.13	3521	1501	2020
28	Vanapuram	12.10	79.03	3807	2219	1588
29	Velunganandal	12.36	79.14	3521	1568	1953
30	Velunganandal	12.37	79.14	3322	1963	1359
31	Vilanallur	12.58	79.50	3521	1587	1934

Table 6. Block wise spatial estimation of potential, actual yield and Yield gap of Peanut at Thiruvannamali district of Tamil Nadu during *Rabi* 2020-21.

Sl. No.	Block Name	Spatial Potential Yield (Kg/ha)			Spatial Actual Yield (Kg/ha)			Spatial Yield Gap (Kg/ha)		
		Minimum	Maximum	Mean	Minimum	Maximum	Mean	Minimum	Maximum	Mean
1	Anakkavur	3723	3964	3867	1421	1903	1726	2034	2326	2140
2	Arani	3718	3980	3847	1401	1934	1692	1991	2322	2155
3	Chengam	3744	4140	3878	1457	2223	1747	1778	2365	2131
4	Chetpet	3774	4005	3883	1540	1979	1756	1962	2274	2127
5	Cheyyar	3758	3960	3862	1527	1897	1718	1995	2286	2143
6	Jawadhu hills	3821	3964	3879	1644	1904	1750	1976	2238	2131
7	Kalasapakam	3764	3976	3880	1541	1926	1752	1960	2310	2128
8	Keelpennathur	3716	4111	3882	1437	2172	1755	1890	2370	2127
9	Peranamallur	3711	3984	3864	1397	1940	1723	1944	2345	2141
10	Polur	3805	3977	3878	1570	1927	1748	1983	2287	2130
11	Pudupalayam	3748	4004	3877	1512	2153	1745	1740	2335	2131
12	Thandrampet	3724	4306	3877	1394	2526	1746	1514	2460	2131
13	Thellar	3765	3977	3877	1561	1927	1747	2030	2231	2131
14	Thurinjapuram	3750	4039	3887	1516	2187	1765	1733	2307	2123
15	Thiruvannamalai	3753	4250	3885	1517	2423	1761	1456	2508	2124
16	Vandavasi	3753	3978	3871	1469	1929	1734	1976	2335	2136
17	Vembakkam	3752	3936	3863	1434	1858	1720	2072	2234	2143
18	West arani	3721	3975	3868	1461	1925	1729	1994	2299	2139
Total / Mean		3750	4029	3874	1489	2041	1740	1890	2324	2134

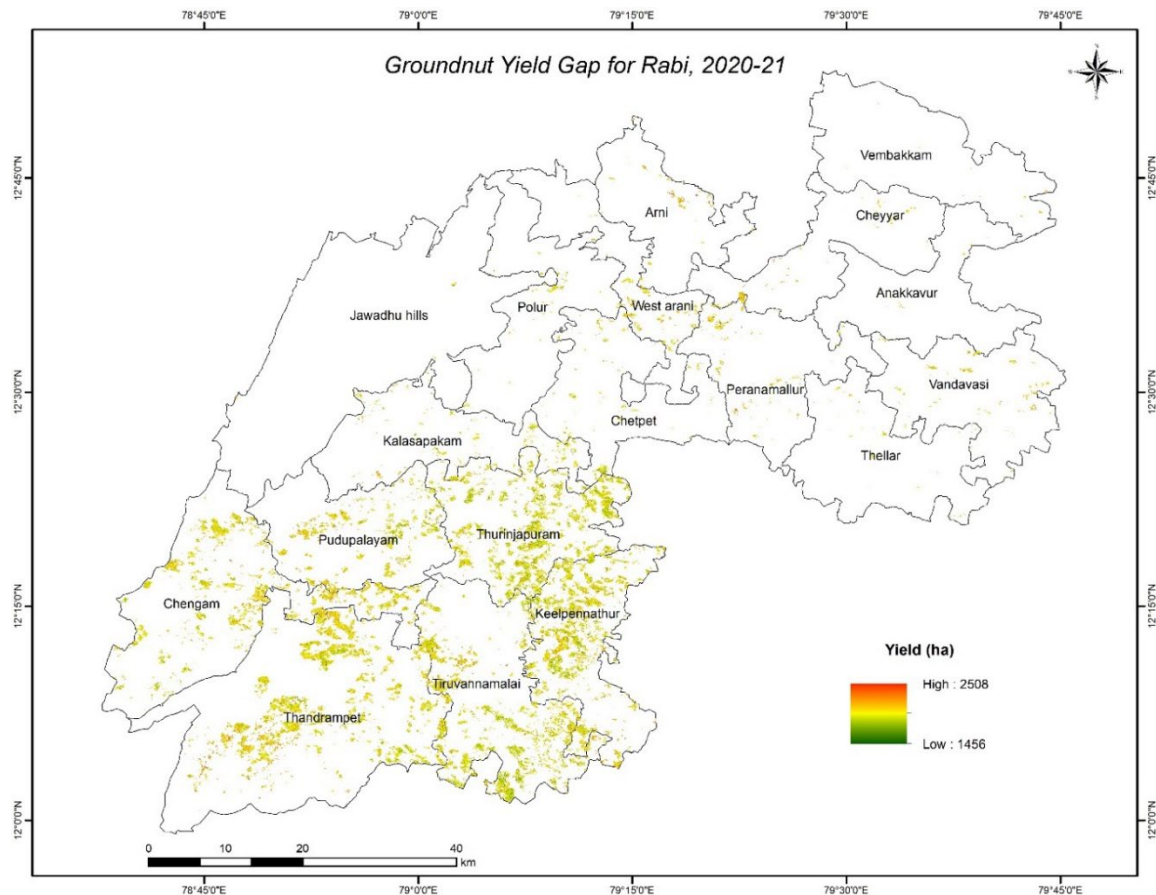


Figure 10. Spatial yield gap of Peanut at Thiruvannamalai district during Rabi 2020-21.

4. Conclusion

Integration of SAR Sentinel-1A with CROPGRO Peanut for Spatial yield gap assessment of Peanut during Rabi 2020-21 at Thiruvannamalai district had shown that 2134 kg/ha of average spatial yield gap with mean minimum of 1890 kg/ha and maximum of 2324 kg/ha. The key production constraints of this Peanut growing areas in Tamil Nadu was due to seasonal rainfall unpredictability, poor soil fertility, lack of improved varieties, and inadequate weed management, which created a wide gap between potential and attainable yield. The current yield gap could be bridged by combining traditional agronomic approaches and latest technologies with the involvement of different stakeholders. As a result, remote sensing to examine the magnitude and causes of yield gaps on a regular basis with improved yield gap awareness will be critical in satisfying future crop demand at reasonable prices while minimizing the environmental effect.

Author Contributions: All the authors (ST, SP, NSS, KR, RK and MR) have contributed substantially to this manuscript. Conceptualization, SP.; methodology, KR and RK; validation, ST and NSS; formal analysis, ST and NSS investigation, SP, KR and RK.; writing-original draft preparation, ST, NSS and GS; writing-review and editing, SP, KR, RK and MR; supervision, SP and KR.; funding acquisition, SP, KR and RK. All authors have read and agreed to the published version of the manuscript.

Acknowledgments: The authors acknowledge the Agriculture and Land Eco system Division, Space Application Centre, ISRO, Ahmedabad for providing the funding to carry out the investigation work in a project mode (Space Technology Utilization for Food Security, Agricultural Assessment and Monitoring - SUFALAM Project). They also acknowledge the Professor and Head, staffs of the Department of Remote Sensing and GIS, TNAU for their invaluable assistance, comments, and constructive suggestions on the research and manuscript. We also like to thank everyone who provided technical assistance during the study's execution.

Conflicts of Interest: The authors declare no conflict of interest.

Appendix 1

Prevailed soil series informations of Thiruvannamalai district used in S built tool of DSSAT model

Soil Series	Depth	Sand (%)	Silt (%)	Clay (%)	Texture Class	PH	EC	OC (%)	CEC	ESP
Perundurai	13	79.00	6.00	15.00	Sandy loam	6.00	0.25	0.41	10.60	2.74
	38	41.00	11.00	48.00	Clay	5.90	0.22	0.50	22.80	1.32
	70	23.00	8.00	69.00	Clay	5.90	0.18	0.70	26.40	1.52
	92	45.00	9.00	46.00	Clay	6.40	0.18	0.30	19.20	1.61
Devikapuram	14	43.80	21.60	34.60	Clay loam	7.00	0.10	0.52	14.51	0.76
	44	65.80	12.30	21.90	Sandy clay loam	7.30	0.10	0.17	10.23	0.88
	59	64.90	12.80	22.30	Sandy clay loam	7.40	0.10	0.23	11.12	1.08
	79	66.30	16.90	16.80	Sandy loam	7.70	0.10	0.11	8.64	0.69
	98	68.70	7.50	23.80	Sandy clay loam	7.50	0.10	0.20	12.46	0.56
Meyyur	16	51.02	25.17	23.81	Sandy clay loam	8.90	0.40	0.75	39.53	1.10
	30	36.27	32.90	30.83	Clay loam	9.00	0.70	0.78	40.32	1.08
	50	20.21	35.67	44.12	Clay	9.30	1.10	0.80	42.84	1.02
	110	42.39	11.49	46.12	Clay	9.10	0.90	0.65	42.00	1.04
Vetavalam	25	65.12	15.68	19.20	Sandy clay loam	7.20	0.40	0.64	21.94	1.19
	52	73.54	12.26	14.20	Sandy loam	6.90	0.30	0.67	21.41	1.21
Villukam	14	46.72	18.28	35.00	Clay	8.50	1.41	0.31	27.10	2.80
	36	44.41	18.89	36.70	Clay	7.90	0.25	0.32	28.20	1.38
	72	42.11	19.00	38.89	Clay	7.80	0.22	0.30	30.10	1.40
	103	37.34	22.66	40.00	Clay	7.80	0.20	0.25	31.26	1.02
Kollattur	18	64.77	14.34	20.89	Sandy clay loam	6.34	0.05	0.45	11.40	4.91
	47	56.37	3.95	39.68	Sandy clay	6.69	0.04	0.37	13.80	2.90
Ayyalur	16	87.10	8.00	4.90	Loamy sand	6.60	0.02	0.32	10.60	2.08
	40	43.00	17.00	40.00	Clay loam	6.20	0.22	0.17	15.40	1.43
	75	60.36	2.29	37.35	Sandy clay	6.50	0.20	0.28	24.80	0.97
	127	59.90	2.60	37.50	Sandy clay	6.60	0.10	0.17	21.95	1.23
Perumaltangal	14	40.26	23.46	36.28	Clay	7.17	0.16	0.56	22.00	5.83
	51	34.89	24.87	40.24	Clay	7.27	0.13	0.41	25.60	4.88
Matathari	12	12.30	43.20	44.50	Silty clay	8.60	0.30	0.54	23.00	12.61
	25	9.30	44.40	46.30	Silty clay	8.50	0.30	0.43	23.24	8.18
	55	53.20	8.50	38.30	Sandy clay	8.50	0.20	0.38	28.00	6.43
	85	51.80	10.60	37.60	Sandy clay	8.50	0.20	0.34	30.24	5.62
Papperi	12	66.00	13.20	20.80	Sandy clay loam	7.00	0.30	0.30	7.80	25.64
	23	67.50	10.90	21.60	Sandy clay loam	7.00	0.20	0.20	8.80	11.36
	40	66.40	11.20	22.40	Sandy clay loam	7.30	0.20	0.20	7.22	24.93
	85	67.20	11.00	21.80	Sandy clay loam	7.30	0.20	0.20	6.22	25.72
Kalugachalapuram	12	35.00	22.00	43.00	Clay	6.44	0.52	0.84	19.60	5.61
	35	34.00	20.00	46.00	Clay	6.55	0.44	0.62	22.30	7.17
	68	32.00	19.00	49.00	Clay	6.59	0.53	0.60	22.60	5.84
	86	24.60	24.80	50.60	Clay	6.56	0.69	0.58	27.80	4.53
	113	24.40	29.60	46.00	Clay	6.40	0.50	0.52	28.50	3.51

References

1. Chapagain, T. and A. Good. Yield and production gaps in rainfed wheat, barley, and canola in Alberta. *Frontiers in Plant Science*, 2015, 6, 990–999.
2. Hochman, Z.; Gobbett, D.; Horan, H.; Garcia, F.J.N. Data rich yield gap analysis of wheat in Australia. *Field Crop. Res.* 2016, 197, 97–106.
3. Eash L, Fonte SJ, Sonder K, Honsdorf N, Schmidt A, Govaerts B and Verhulst N Factors contributing to maize and bean yield gaps in Central America vary with site and agroecological conditions. *The Journal of Agricultural Science*, 2017, 157, 300–317.
4. Lobell, D.B.; Cassman, K.G.; Field, C.B. Crop yield gaps: Their importance, magnitudes, and causes. *Annu. Rev. Environ. Resour.* 2009, 34, 179–204.
5. Van Ittersum, M.; Cassman, K.G.; Grassini, P.; Wolf, J.; Tittonell, P.; Hochman, Z. Yield gap analysis with local to global relevance—A review. *Field Crop. Res.* 2013, 143, 4–17.
6. Cassman, K. What do we need to know about global food security? *Glob. Food Secur.* 2012, 1, 81–82.
7. Najafi E, Devineni N, Khanbilvardi RM and Kogan F. Understanding the changes in global crop yields through changes in climate and technology. *Earth's Future*, 2016, 6, 410–427.
8. Soltani A, Alimagham SM, Nehbandani A, Torabi B, Zeinali E, Zand E, Vadez VD, Van Loon MP and Van Ittersum MK Future food self-sufficiency in Iran: a model-based analysis. *Global Food Security*, 2020, 24, 100351–100359 (2020).
9. Laborte AG, de Bie K (CAJM), Smalinga EMA, Moya PF, Boling AA and Van Ittersum MK. Rice yields and yield gaps in Southeast Asia: past trends and future outlook rice yields and yield gaps in Southeast Asia: past trends and future outlook. *European Journal of Agronomy*, 2012, 36, 9–20.
10. FAO and DWFI. Yield Gap Analysis of Field Crops –Methods and Case Studies, by Sadras VO, Cassman KGG, Grassini P, Hall AJ, Bastiaanssen WGM, Laborte AG, Milne AE, Sileshi G and Steduto P. 2015, FAO Water Reports No. 41, Rome, Italy.
11. Paul, G.C.; Saha, S.; Hembram, T.K. Application of phenology-based algorithm and linear regression model for estimating rice cultivated areas and yield using remote sensing data in Bansloi River Basin, Eastern India. *Remote Sens. Appl. Soc. Environ.* 2020, 19, 100367.
12. Deka, R.L.; Hussain, R.; Singh, K.K.; Rao, V.U.M.; Balasubramaniam, R.; Baxla, A.; Rao, V.; Balasubramaniam, R. Rice phenology and growth simulation using CERES-rice model under the agro-climate of upper brahmaputra valley of Assam. *Mausam* 2016, 67, 591–598.
13. Dwivedi, M.; Saxena, S.; Ray, S.S. Assessment of rice biomass production and yield using semi-physical approach and remotely sensed data. *Int. Arch. Photogramm. Remote Sens. Spat. Inf. Sci.* 2019, 42, 217–222.
14. Lobell, D.B. The use of satellite data for crop yield gap analysis. *Field Crops Res.*, 2013, 143, 56–64. doi:10.1016/j.fcr.2012.08.008.
15. Soltani A and Sinclair TR. Modeling Physiology of Crop Development, Growth and Yield. Oxfordshire, UK or Cambridge, MA, USA: CABI, 2012.
16. Eitzinger J, Thaler S, Schmid E, Strauss F, Ferrise R, Moriondo M, Bindi M, Palosuo T, Rötter R, Kersebaum KC, Olesen JE, Patil RH, Aylan LS, Çaldag B and Çaylak O. Sensitivities of crop models to extreme weather conditions during flowering period demonstrated for maize and winter wheat in Austria. *Journal of Agricultural Science*, 2013, 151, 813–835.
17. Batchelor, W. D., B. Basso, and J. O. Paz. Examples of strategies to analyze spatial and temporal yield variability using crop models. *European J. Agron.* 2002, 18(2): pp. 141–158.
18. Xie, Y., Z. Sha, and M. Yu. Remote sensing imagery in vegetation mapping: A review. *J. Plant Ecology* 1(1): pp. 9–23 (2008).
19. Burke, M.; Lobell, D.B. Satellite-Based Assessment of Yield Variation and Its Determinants in Smallholder African Systems. *Proc. Natl. Acad. Sci. USA*, 2017, 114, 2189–2194.
20. Inoue, Y. Synergy of remote sensing and modeling for estimating ecophysiological processes in plant production. *Plant Production Sci.*, 2003, 6(1): pp. 3–16.
21. Dorigo, W. A., R. Zurita-Milla, A. J. W. de Wit, J. Brazile, R. Singh, and M. E. Schaepman. A review on reflective remote sensing and data assimilation techniques for enhanced agroecosystem modeling. *Intl. J. Applied Earth Observation and Geoinformation*, 2007, 9(2): pp. 165–193.
22. Adhikari, K., F. Carre, G. Toth. Site-specific Land Management General Concepts and Applications; European Commission, Luxembourg: Luxembourg, 2009.
23. Sadras, V.O., Cassman, K.G., Grassini, P., Hall, A.J., Bastiaanssen, W.G.M., Laborte, A.G., Milne, A.E., Sileshi, G., Steduto, P. Yield Gap Analysis of Field Crops: Methods and Case Studies; Eds.; FAO Water Reports No. 41; FAO: Rome, Italy, 2015.
24. Holecz, F, M Barbieri, F Collivignarelli, L Gatti, A Nelson, TD Setiyono, M Boschetti, G Manfron, PA Brivio, and J Quilang. 2013. "An operational remote sensing based service for rice production estimation at national scale." Proceedings of the living planet symposium.

25. Lillesand, TM. "Strategies for improving the accuracy and specificity of large-area, satellite-based land cover inventories." *International Archives of Photogrammetry and Remote Sensing*, 1994 30:23-30.
26. Congalton, RG. "A review of assessing the accuracy of classifications of remotely sensed data." *Remote Sensing of Environment*, 1991, 37 (1):35-46.
27. Richards, JA. 1993. "Sources and characteristics of remote sensing image data." In *Remote Sensing Digital Image Analysis*, 1-37. Springer. <https://link.springer.com/book/10.1007/978-3-642-88087-2>
28. Deiveegan, M., S. Pazhanivelan, K.P. Ragunath and R. Kumaraperumal. Detection of Agricultural Vulnerability to Drought Using NDVI and Land Surface Temperature in Salem and Namakkal districts of Tamil Nadu. *Advances in Life Sciences*, 2016, 5(17), 6868- 6873.
29. Venkatesan. M., Pazhanivelan. S., Sudarmanian. N. S. Multi-Temporal Feature Extraction for Precise Maize Area Mapping Using Time-Series Sentinel 1A SAR Data. *The International Archives of the Photogrammetry, Remote Sensing and Spatial Information Sciences*, 2019, Vol. XLII-3/W6.
30. Sudarmanian, NS. S Pazhanivelan, KP Ragunath and S Panneerselvam. Estimation of methane emission from rice fields using satellite data in Thiruvavur district. *Madras Agricultural Journal*, 2019, 7(3): 4116-4120.
31. Pazhanivelan, S.; Geethalakshmi, V.; Tamilmounika, R.; Sudarmanian, N.S.; Kaliaperumal, R.; Ramalingam, K.; Sivamurugan, A.P.; Mrunalini, K.; Yadav, M.K.; Quicho, E.D. Spatial Rice Yield Estimation Using Multiple Linear Regression Analysis, Semi-Physical Approach and Assimilating SAR Satellite Derived Products with DSSAT Crop Simulation Model. *Agronomy* 2022, 12, 2008. <https://doi.org/10.3390/agronomy12092008>
32. Chisanga, CB, E Phiri, and V Chinene. 2021. "Evaluating APSIM-and-DSSAT-CERES-Maize Models under Rainfed Conditions Using Zambian Rainfed Maize Cultivars." *Nitrogen*, 2021, 2 (4):392-414.
33. Yadav, S, H Patel, G Patel, M Lunagaria, B Karande, A Shah, and V Pandey. 2012. "Calibration and validation of PNUTGRO (DSSATv4.5) model for yield and yield attributing characters of kharif Peanut cultivars in middle Gujarat region." *Journal of Agrometeorology*, 2012, Special (14):24-29.
34. Parmar, P, HR Patel, SB Yadav, and V Pandey. "Calibration and validation of DSSAT model for kharif Peanut in North-Saurashtra agro-climatic zone of Gujarat." *Journal of Agrometeorology*, 2013, 15 (1):62.
35. Naab, J, K Boote, J Jones, and CH Porter. 2015. "Adapting and evaluating the CROPGRO-peanut model for response to phosphorus on a sandy-loam soil under semi-arid tropical conditions." *Field Crops Res.* 2015, 176:71-86.
36. Halder, D, RK Panda, RK Srivastava, and S Kheroar. 2017. "Evaluation of the CROPGRO-Peanut model in simulating appropriate sowing date and phosphorus fertilizer application rate for peanut in a subtropical region of eastern India." *The Crop Journal* 5 (4):317-325.
37. Gilbert, R, K Boote, and J Bennett. "On-farm testing of the PNUTGRO crop growth model in Florida." *Peanut Science*, 2002, 29 (1):58-65.
38. Pandey, V, A Shekh, R Vadodaria, and B Bhatt. "Evaluation of CROPGRO peanut model for two genotypes under different environment." *National seminar on Agro Meteorological Research for Sustainable Agricultural Production at GAU Anand*, 2001.
39. Garcia, AG, G Hoogenboom, LC Guerra, JO Paz, and CW Fraisse. 2006. "Analysis of the inter-annual variation of peanut yield in Georgia using a dynamic crop simulation model." *Transactions of the ASABE*, 2006, 49 (6):2005-2015.
40. Biswal, A, B Sahay, K Ramana, S Rao, and MS Sai. "Relationship between AWiFS derived Spectral Vegetation Indices with Simulated Wheat Yield Attributes in Sirsa district of Haryana." *The International Archives of Photogrammetry, Remote Sensing and Spatial Information Sciences*, 2014, 40 (8):689.
41. Bhatia, V, P Singh, S Wani, and K Srinivas. "Yield gap analysis of Peanut in India using simulation modeling." *Global theme on Agro ecosystems Report:43*. 2005. https://www.iwmi.cgiar.org/assessment/files_new/publications/ICRISATReportNo_31.
42. Anothai, J, A Patanothai, K Pannangpetch, S Jogloy, K Boote, and G Hoogenboom. "Multi-environment evaluation of peanut lines by model simulation with the cultivar coefficients derived from a reduced set of observed field data." *Field Crops Research*, 2009, 110 (2):111-122.
43. Putto, C, A Patanothai, S Jogloy, K Pannangpetch, K Boote, and G Hoogenboom. 2009. "Determination of efficient test sites for evaluation of peanut breeding lines using the CSM-CROPGRO-peanut model." *Field Crops Research*, 2009, 110 (3):272-281.
44. Maloom, J.M.; Saludes, R.B.; Dorado, M.A.; Cruz, P.C.S. Development of a GIS-Based Model for Predicting Rice Yield. *Philipp. J. Crop Sci.* 2014, 39, 8–19.

-
45. Hoogenboom G, Porter CH, Boote KJ, Shelia V, Wilkens PW, Singh U, White JW, Asseng S, Lizaso JJ, Moreno LP, Pavan W, Ogoshi R, Hunt LA, Tsuji GY and Jones JW. The DSSAT crop modeling ecosystem. In Boote KJ (ed.), *Advances in Crop Modeling for a Sustainable Agriculture*. Cambridge: Burleigh Dodds Science Publishing, 2019, pp. 173-216.
 46. Shiferaw W and Yoseph T. Collection, characterization and evaluation of sorghum (*Sorghum bicolor* (L.) Moench) landraces from South Omo and Segen people's zone of South Nation Nationality Peoples Region, Ethiopia. *International Research Journal of Agricultural Science and Soil Science*, 2014, 4, 76–84.